Bioorganic & Medicinal Chemistry 20 (2012) 7139–7148

Contents lists available at SciVerse ScienceDirect

Bioorganic & Medicinal Chemistry

journal homepage: www.elsevier.com/locate/bmc

# DNA binding acridine–thiazolidinone agents affecting intracellular glutathione

Helena Paulíková [a,*], Zuzana Vantová [a,b], Ľuba Hunáková [e], Lýdia Čižeková [a], Mária Čarná [a], Mária Kožurková [c], Danica Sabolová [c], Pavol Kristian [d], Slávka Hamuľaková [d], Ján Imrich [d]

[a] Department of Biochemistry and Microbiology, Faculty of Chemical and Food Technology, Faculty of Chemical and Food Technology, Radlinského 9, SK-81237 Bratislava, Slovak Republic
[b] Department of Chemical and Biochemical Engineering, Faculty of Chemical and Food Technology, Faculty of Chemical and Food Technology, Radlinského 9, SK-81237 Bratislava, Slovak Republic
[c] Department of Biochemistry, Institute of Chemistry, Faculty of Science, P.J. Šafárik University, Moyzesova 11, SK-04167 Košice, Slovak Republic
[d] Department of Organic Chemistry, Institute of Chemistry, Faculty of Science, P.J. Šafárik University, Moyzesova 11, SK-04167 Košice, Slovak Republic
[e] Cancer Research Institute, Vlárska 7, SK-81237 Bratislava, Slovak Republic

ARTICLE INFO

*Article history:*
Received 12 July 2012
Revised 21 September 2012
Accepted 26 September 2012
Available online 12 October 2012

*Keywords:*
Acridine
DNA-intercalation
Glutathione
Antitumor

ABSTRACT

Three new acridine–thiazolidinone derivatives (**2a**–**2c**) have been synthesized and their interactions with calf thymus DNA and a number of cell lines (leukemic cells HL-60 and L1210 and human epithelial ovarian cancer cell lines A2780) were studied. The compounds **2a**–**2c** possessed high affinity to calf thymus DNA and their binding constants determined by spectrofluorimetry were in the range of $1.37 \times 10^6$–$5.89 \times 10^6$ $M^{-1}$. All of the tested derivatives displayed strong cytotoxic activity in vitro, the highest activity in cytotoxic tests was found for **2c** with $IC_{50} = 1.3 \pm 0.2$ μM (HL-60), $3.1 \pm 0.4$ μM (L1210), and $7.7 \pm 0.5$ μM (A2780) after 72 h incubation. The cancer cells accumulated acridine derivatives very fast and the changes of the glutathione level were confirmed. The compounds inhibited proliferation of the cells and induced an arrest of the cell cycle and cell death. Their influence upon cells was associated with their reactivity towards thiols and DNA binding activity.



## 1. Introduction

Antitumor effects of acridines are associated not only with their interaction with DNA but also with proteins, especially some key enzymes important in cell proliferation as topoisomerases or telomerases.[1–3] Acridines can interact with DNA either via intercalation or groove-binding and may thus block a DNA replication, transcription, or DNA repair.[4] In the meantime, the best known acridine drugs used in antitumor therapy are amsacrine and DACA. Damage of DNA by these compounds is usually strengthened by the oxidative stress.[5] The search for novel anticancer drugs encourages also syntheses of new acridine derivatives.[6–8] Several series of novel 9- and 3,6-substituted acridines have recently been prepared in our laboratory and investigated for their DNA binding properties and in vitro antineoplastic activity.[9–13] Besides antitumor effects found at micromolar concentrations, all new substances displayed a potent DNA binding with binding constants in the range of $10^5$–$10^6$ $M^{-1}$. This affinity as well as UV–vis, spectrofluorimetric and CD studies confirmed an intercalation of our ligands into DNA to be a principal mode of interaction.

In search for new pharmacophoric structures we were inspired by acridine–thiazolidinone derivatives such as methyl [2-(acridin-9-ylimino)-3-substituted-4-oxo-thiazolidin-5-ylidene]acetate which were synthesized recently by our group from 1-alkyl(acyl)-4-(acridin-9-yl)thiosemicarbazides and dimethyl acetylenedicarboxylate (DMAD).[14–17] The present study was designed to expand our knowledge of the mechanism of cytotoxicity of related acridine–thiourea derivatives which possess also reactivity towards thiols. Three new acridine–thiazolidinone derivatives were prepared from *N*-(acridin-9-yl)-*N*′-substituted thioureas (R = *sec*-butyl, *tert*-butyl, and 4-bromophenyl) and DMAD and their DNA binding activity was evaluated. Although, anticancer activity of acridines is mainly related to their capacity to bind to DNA, the cytotoxicity of these may be enhanced by an increase of their electrophilicity to facilitate the reaction with essential SH groups present in living organisms, especially a main low-molecular thiol, glutathione. Reactivity of acridines with sulfhydryls could modify SH-proteins and alter intracellular glutathione redox status, which modulates a lot of cellular events, for example, selective gene expression, DNA synthesis, or regulation of the cell cycle.[18–20] In vitro cytotoxic effects of these compounds on murine leukemic cells L1210, human promyelocytic leukemic HL-60 cells, and A2780 human ovarian adenocarcinoma cells were monitored. To investigate the mechanism of cytotoxicity, a cellular accumulation of acridine–thiazolidinone derivatives was studied and their influence on the intracellular glutathione level was evaluated. The cell death and changes in the cell cycle were observed.

* Corresponding author.
*E-mail address:* helena.paulikova@stuba.sk (H. Paulíková).

0968-0896/$ - see front matter © 2012 Elsevier Ltd. All rights reserved.
http://dx.doi.org/10.1016/j.bmc.2012.09.068

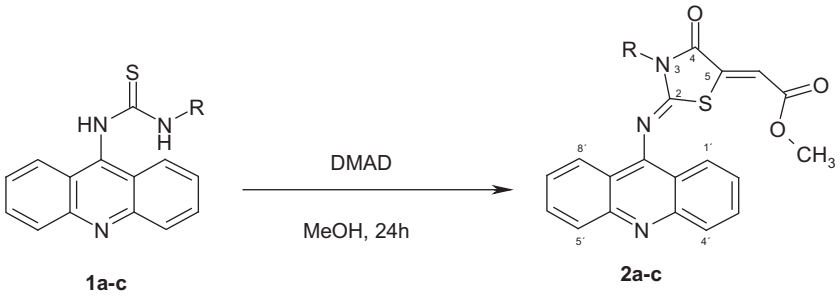


**Scheme 1.** Synthesis of tested compounds **2a**–**2c**.

## 2. Results and discussion

### 2.1. Chemistry

Three new derivatives were prepared from *N*-(acridin-9-yl)-*N*′-substituted thioureas (R = *sec*-Bu (a), *tert*-Bu (b), 4-Br-Ph (c)) and DMAD (Scheme 1).

To a stirred solution of corresponding *N*-(acridin-9-yl)-*N*′-substituted thiourea **1** (5 mmol) in methanol (30 mL), DMAD (6 mmol) was added and the solution was stirred for 20–24 h at room temperature.[21,22] The reaction course was followed by TLC, the eluent benzene/acetone, 9:1. The crude product was isolated by evaporation of the solvent, purified by column chromatography on silica gel using the same eluent as above and obtained as pale yellow crystals.

### 2.2. DNA binding studies

Acridine intercalation into DNA, a strong stacking interaction between an aromatic chromophore of the ligand and DNA base pairs, is characteristic of a hypochromism and red shifts in the UV–vis spectra.[23–25] Interaction of ligands **2a**–**2c** with calf thymus (ct) DNA was therefore examined by UV–vis, fluorimetric titrations, and thermal melting experiments. UV–vis data of compounds **2a**–**2c** are displayed in Table 1 and absorption spectra of **2c** in the absence and presence of calf thymus DNA are shown in Figure 1. The spectra show a significant absorption in the range of 300–600 nm, typical for transitions between π-electron energy levels of the acridine ring. As the DNA concentration increased, the bands showed moderate hypochromicities (21.5–35.9%) and slight bathochromic shifts which indicate an insertion of the compounds into DNA. The overall changes in the UV–vis spectra suggest that intercalation is the dominant binding mode.

DNA binding properties of compounds **2a**–**2c** were also evaluated by thermal melting experiments where duplex DNA was thermally denatured into single-stranded components in the presence and absence of these ligands. The DNA helix denaturation can be determined by monitoring a change of the DNA absorbance at 260 nm as a function of temperature. The DNA melting temperatures ($T_m$) in the presence and absence of studied derivatives **2a**–**2c** are shown in Table 1. The $T_m$ of free ctDNA was 70.5 °C and increased to 74–81 °C upon **2a**–**2c** intercalative binding in accord with literature.[10]

**Table 1**
UV–vis absorption data of acridine derivatives **2a**–**2c**

| Compound | $\lambda_{max}$ free (nm) | $\lambda_{max}$ bound (nm) | $\Delta\lambda$ (nm) | Hypochromicity (%) | [a]$T_m$ (°C) |
|---|---|---|---|---|---|
| **2a** | 326 | 331 | 5 | 26.3 | 75 |
| **2b** | 324 | 333 | 9 | 31.2 | 74 |
| **2c** | 326 | 330 | 4 | 24.2 | 81 |

[a] $T_m$ was measured in BPE buffer (6 mM $Na_2HPO_4$, 2 mM $Na_2HPO_4$, 1 mM EDTA), pH 7.1.

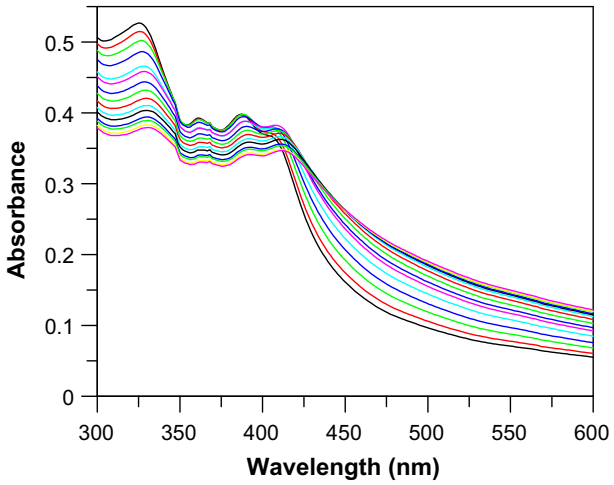


**Figure 1.** UV–vis spectral changes of **2c** (25 μM) upon addition of ctDNA (from top to bottom 0–30 μM bp) in 0.01 M Tris (pH 7.4), 24 °C.

In a spectrofluorimetric study, free **2a**–**2c** exhibited a broad emission band in the range of 420–550 nm. Excitation wavelength was set to 384 nm and the spectra were monitored at fixed drug concentration 26.7 μM. Titration with increasing concentration of ctDNA continued until no further changes in the spectra of the drug–DNA complexes were recorded (Fig. 2). Binding of the acridine probes into DNA helix was found to reduce the fluorescence of studied acridine derivatives and represents another independent proof of intercalation.

The binding constants *K* of **2a**–**2c** with ctDNA determined by spectrofluorimetry were calculated according to a McGhee and von Hippel method.[26,27] Their large values in the range of $1.37 \times 10^6$–$5.89 \times 10^6$ $M^{-1}$ increased in the order **2b** < **2a** < **2c** and are indicative of a high affinity of the acridine chromophore to DNA-base pairs (see Table 2). The binding affinity is approximately ten-times higher than *K* values of related acridine-*bis*-imidazolidinone intercalators ($1.9 \times 10^5$–$7.1 \times 10^5$ $M^{-1}$)[9] derived from proflavine (acridine-3,6-diamine), daunomycin ($7.09 \times 10^5$ $M^{-1}$), or acridine orange ($3.19 \times 10^5$ $M^{-1}$),[28] even two-order magnitudes higher than those of acridine-*bis*-thiazolidinones ($2.2$–$6.2 \times 10^4$ $M^{-1}$).[12] These data clearly show that less bulky mono-9-substituted acridine–thiazolidinones studied here are better suited for intercalative (threading) binding than bis-3,6-substituted proflavine derivatives. Accordingly, as we have proven

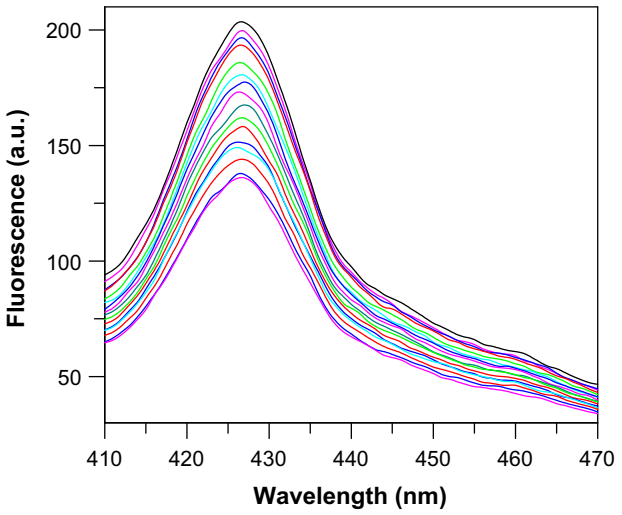


**Figure 2.** Spectrofluorimetric titration of derivative **2c** (26.7 μM) in 0.01 M Tris buffer (pH 7.4, 24 °C) by increasing concentration of ctDNA (from top to bottom, 0–32 μM bp, at 2 μM intervals), $\lambda_{ex}$ = 384 nm.

**Table 2**
Fluorescence data of compounds **2a**–**2c**

| Compound | $\lambda_{em}$ (nm) | $\Phi_f$[a] | $K \times 10^6$ ($M^{-1}$) |
|---|---|---|---|
| **2a** | 421 | 0.61 | 2.21 ± 0.25 |
| **2b** | 422 | 1.00 | 1.37 ± 0.13 |
| **2c** | 425 | 0.75 | 5.89 ± 0.81 |

[a] Relative fluorescence intensity was calculated using the compound **2b** as a standard ($\Phi_f' = 1$).

**Table 3**
Cytotoxicity of derivatives **2a**–**2c** against leukemic and A2780 cells—MTT-assay

| Compound | $IC_{50}$ (μM) | | | | | |
|---|---|---|---|---|---|---|
| | HL-60 | | L1210 | | A2780 | |
| | 48 h | 72 h | 48 h | 72 h | 48 h | 72 h |
| **2a** | 3.4 ± 0.5 | 2.1 ± 0.3 | 3.3 ± 0.5 | 7.5 ± 0.7 | 20.8 ± 1,3 | 12.6 ± 1.1 |
| **2b** | 5.4 ± 0.7 | 3.7 ± 0.6 | 17.9 ± 2.2 | 20.9 ± 1.9 | >30 | 23.7 ± 2.8 |
| **2c** | 1.4 ± 0.3 | 1.3 ± 0.2 | 1.7 ± 0.4 | 3.1 ± 0.4 | 12.5 ± 0.2 | 7.7 ± 0.5 |
| **Cisplatin** | ND | 2.2 ± 0.3 | ND | 1.3 ± 0.3 | ND | 2.73 ± 0.6 |

by molecular dynamics calculations of binding energies,[9] preferential mode of DNA binding of proflavine derivatives is a minor-groove binding, not a threading binding as in this case. The reasons for that may be looked for in an electrostatic energy change and entropy decrease accompanying the DNA–ligand binding.[9]

### 2.3. Cytotoxicity of 2a–2c

We performed also a basic pre-screening of cytostatic parameters of derivatives **2a**–**2c**. Leukemic cells HL-60 (human) and L1210 (mice) and human epithelial ovarian cancer cell lines A2780 were treated with derivatives **2a**–**2c** in a concentration range of 0.25–10 μM on the leukemic cells and in the range of 1.0–50 μM on A2780 cells for 3 days. $IC_{50}$ values were determined using a MTT-assay (Table 3). All derivatives displayed inhibitory effect with respect to the control. The most potent cytotoxic derivative was **2c** and the A2780 cell line was less sensitive to cytotoxic action of **2a**–**2c** than leukemic cells.

When compared with cisplatin, the cytotoxicity of our compounds **2a**–**2c** was lower against L1210 and A2780 and similar against HL-60 cells (Table 3). All **2a**–**2c** were less cytotoxic against HL-60 cells than amsacrine ($IC_{50}$ = 0.08 μM, 72 h).[37]

The cytotoxicities of the substances **2a**–**2c** were verified by a direct cell counting method (DCC) using a trypan blue exclusion test. Growth curves of the HL-60 cells were obtained by dye exclusion tests (Fig. 3) and from these $IC_{50}$ values were calculated. All derivatives displayed an inhibitory effect with respect to the control.

When longer-term experiments to determine $IC_{50}$ (72 h) are employed one should remember that several divisions of cultured cells have been completed at the end and repair mechanisms lowering the therapeutic effect may be running. In our case, luckily, the $IC_{50}$ values did not deteriorate upon long-term incubation confirming a persisting prolonged cytotoxicity of **2a**–**2c** on the studied HL-60 cells (Table 4).

The cytotoxicity of **2a**–**2c** against NIH-3T3 mouse embryonic fibroblast cells has been examined. Cytotoxicity of **2c** against NIH-3T3 cells ($IC_{50}$ = 3.5 μM, 72 h) was lower than toxicity against leukemia cells (L1210 or HL-60) but higher than toxicity against A2780 cells.

### 2.4. Accumulation of 2a–2c in the cells

Cells were incubated with **2a**–**2c** at 37 °C for 4 h, washed with PBS, and monitored by fluorescence microscopy. In the control experiment, cells were not treated (data not presented). Leukemic cells accumulated acridine derivatives **2a**–**2c** already after 4 h incubation. As revealed in Figure 4, HL-60 cells became bright-blue about 4 h after addition of all tested derivatives. The rapid internalization of **2a**–**2c** was shown also for A2780 (not shown).

An intracellular uptake of **2c** was confirmed by HPLC. A well-resolved peak that corresponds to **2c** was achieved on a C18 column using the mobile phase consisting of ammonium formate (150 mM) in 80% methanol with pH adjusted to 4.5 using formic acid. The detection of **2c** was carried out at wavelength 370 nm (Fig. 5A, **2c** (1 nmol) was injected). HL-60 cells were incubated with the substance for 10 or 60 min, then cells were washed twice with PBS, extracted with methanol, and the extract was analyzed (Fig. 5B and C). HPLC chromatograms showed that **2c** ($R_t$ = 32.8 min) was accumulated in cells already after 10 min incubation. The level of **2c** did not change after 60 min incubation.

### 2.5. SH-reactivity of 2a–2c and changes of intracellular level of glutathione

It is known that high degree of SH-reactivity is the shared feature of a variety of anticancer agents. Cysyk et al. reported that amsacrine was able to create GSH-acridine thioether conjugate.[30] Accordingly, a similar metabolic transformation of **2a**–**2c** may be expected also here. Although their cytotoxic effect should be associated mainly with their DNA binding activity, these compounds possessing at least five electrophilic $sp^2$ carbons can also interact with intracellular thiols to afford several target structures. To confirm such an assumption, we studied an interaction with a model thiolate, *N*-acetyl-L-cysteine (NAC). UV–vis spectrophotometric analysis (Fig. 6) confirmed that **2c** reacted with NAC to provide a NAC-**2c** conjugate which displayed a distinctly different absorbance spectrum compared to that of the **2c**. An attempt to render an NMR proof of the conjugate structure was precluded by a very different solubility of both reagents not allowing to see sufficient concentrations of the product(s) with supposed limited stability in the reaction mixture.

Moreover, in a following kinetic study, second-order rate constants of the reaction of **2c** with *N*-acetyl-L-cysteine (Table 5) increased in the range of ca. one order of magnitude upon the pH

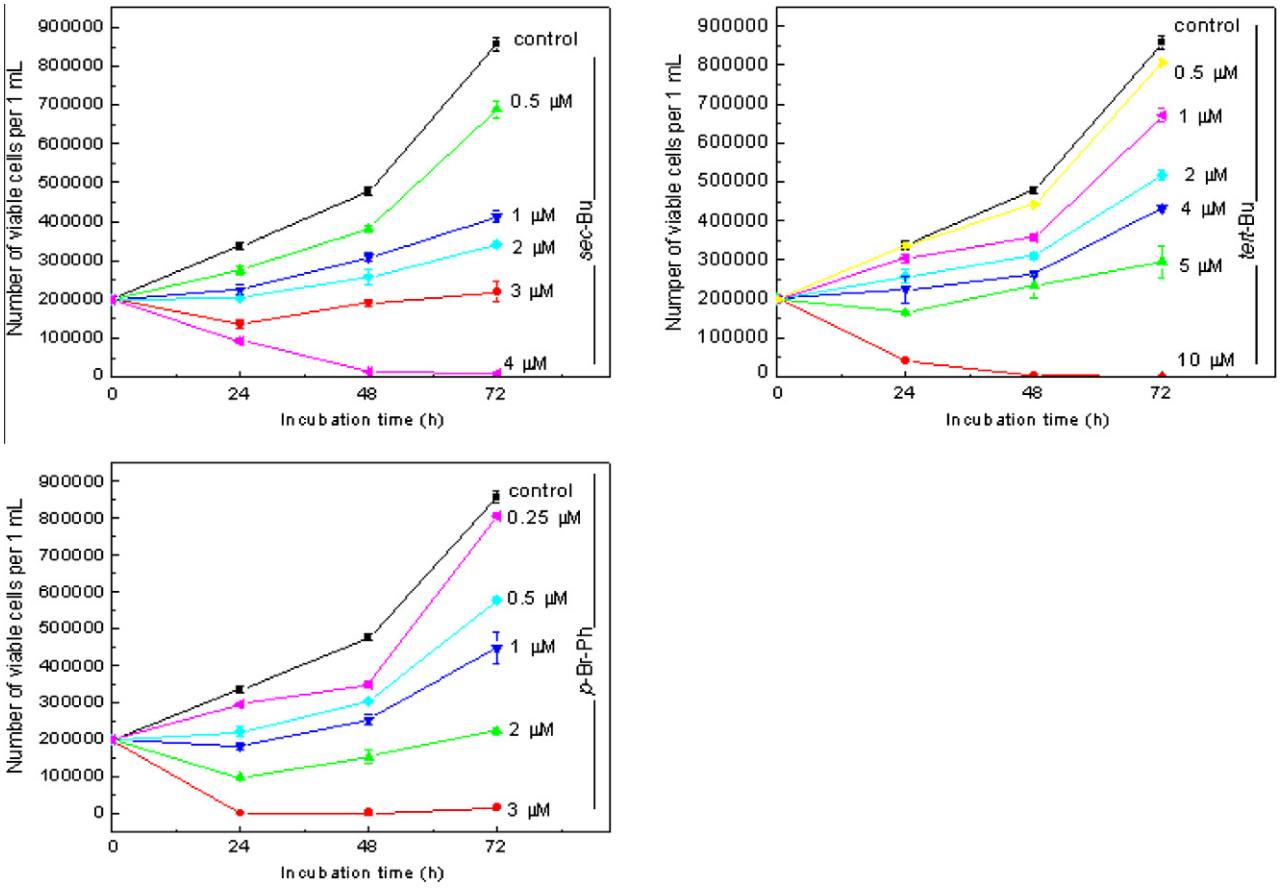


**Figure 3.** Inhibitory effects of derivatives **2a**–**2c** on the proliferation of HL-60 cells. Three-day cell growth is shown in the presence of **2a**–**2c** derivatives: **2a**—*sec*-Bu, **2b**—*tert*-Bu, **2c**—*p*-Br-Ph. Viability of cells was measured by a dye exclusion test using trypan blue. Cells were incubated for 0–72 h without (control) or with 0–10 μM of the compound. Results are expressed as a mean ± S.D. ($n = 3$).

**Table 4**
Cytotoxicity of derivatives **2a**–**2c** against human leukemic cells HL-60—DCC method

| Compound | $IC_{50}$ (μM) HL-60 | |
|---|---|---|
| | 48 h | 72 h |
| **2a** | 2.0 ± 0.4 | 1.7 ± 0.4 |
| **2b** | 3.5 ± 0.7 | 2.8 ± 0.5 |
| **2c** | 1.6 ± 0.6 | 0.9 ± 0.1 |

Cells were incubated for 0–72 h without (control) or with 0–10 μM of the compounds **2a**–**2c**. $IC_{50}$ values are concentrations that produced 50% inhibition of the cell viability. Results are expressed as a mean ± S.D. ($n = 3$).

raise from 6.0 to 7.0 confirming thus a kinetic control in the reaction. Such behavior proves that thiol reacts with the acridine derivative in a thiolate form.

Glutathione (GSH) is a dominant non-protein thiol in mammalian cells whose main role is to detoxificate electrophilic xenobiotics.[31] We suppose that compounds **2a**–**2c** could also form conjugates with intracellular GSH (either spontaneously or enzymatically in reactions catalyzed by glutathione-*S*-transferase), even though we did not succeed to confirm them by direct chemical synthesis. Moreover, SH groups of proteins may be also assumed to react with **2a**–**2c**. If GSH traps the electrophilic acridine derivatives, it actually protects SH groups of proteins against binding of **2a**–**2c.**

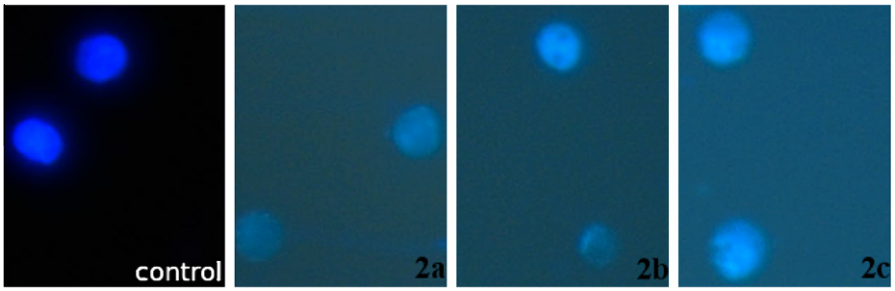


**Figure 4.** Intracellular accumulation of compounds **2a**–**2c** (5 μM each) in HL-60 cells, visualized by fluorescence microscopy after 4 h incubation (magnification 40 × 10). The control was stained with Hoechst 33342.

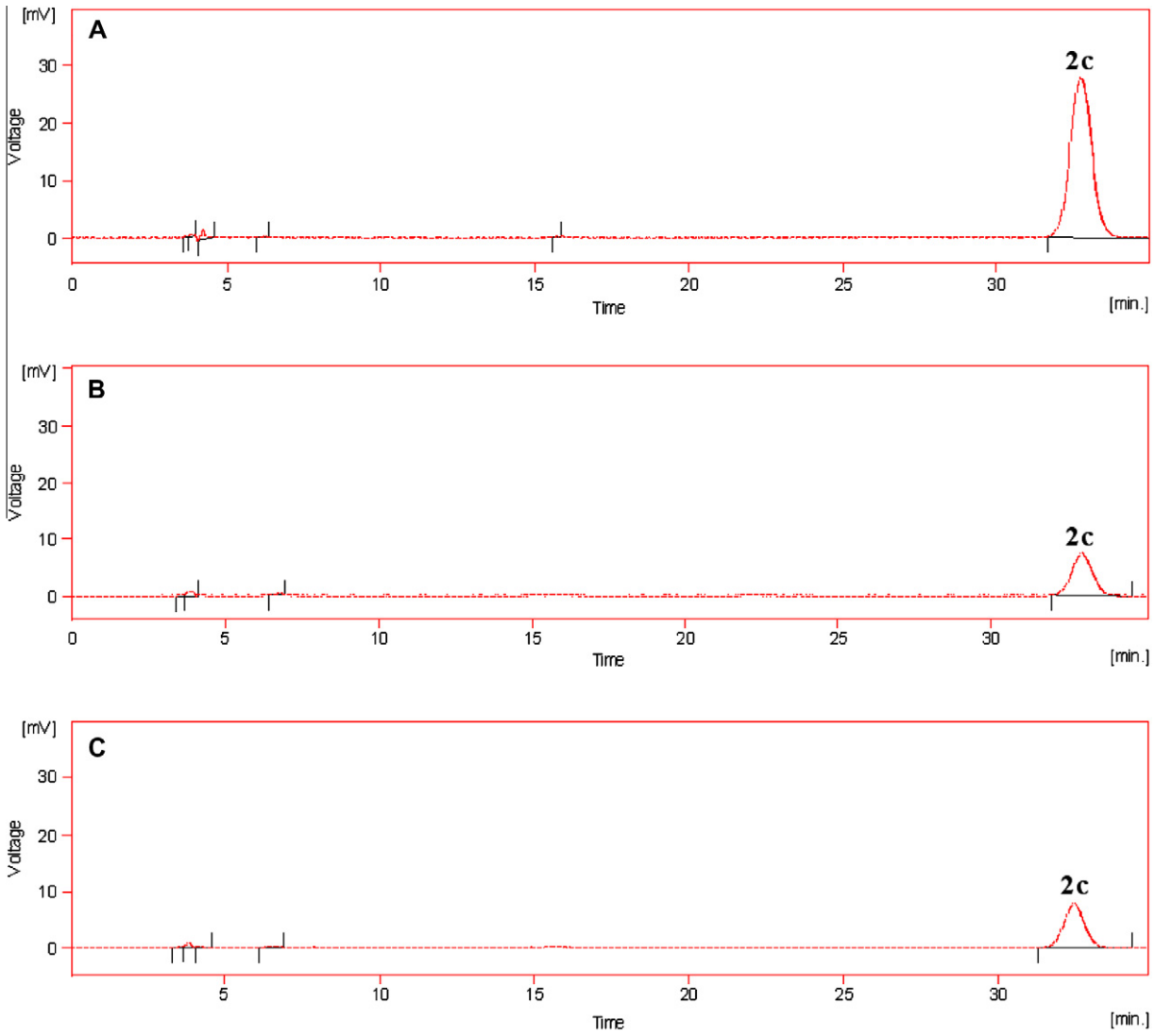


**Figure 5.** HPLC analysis of intracellular accumulation of **2c**. HL-60 cells ($2 \times 10^6$/mL) were incubated with 10 μM **2c** for 10 min (B) and 60 min (C). Standard of **2c** (A) (1 nmol/20 μL) $R_t$ = 32.8 min; $A$ = 1366.622 mV s.

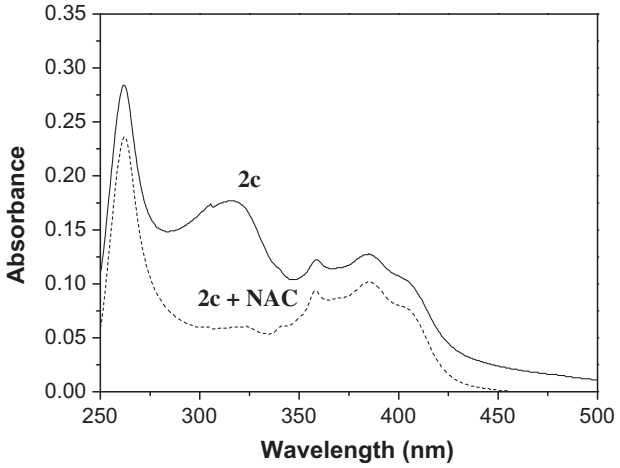


**Figure 6.** The spectral changes observed for **2c** after reaction with NAC. UV–vis spectra: **2c** (solid line) and the spectrum recorded after addition of NAC (dashed line). Spectra were measured in the solution of 50% DMSO and 100 mM Tris/HCl (pH 7) at 25 °C. The mixture of **2c** and NAC was kept at 25 °C for 10 min. The final concentration of **2c** and NAC was 20 μM and 1 mM, respectively.

We therefore examined the level of intracellular glutathione in treated cells. When HL-60 cells were incubated with **2a–2c** for short-time (Fig. 7), the intracellular concentration of GSH (total glutathione) decreased. However, at long-term incubation, the level of intracellular glutathione was recovered, the most with the derivative **2b**. GSH depletion might trigger the downstream events of apoptosis by leaving cells unprotected against thiol oxidation radical production.[32] As seen in Figure 7, the concentration of GSH returned to the control level only in cells incubated with **2b** for 24 h.

**Table 5**
Second-order rate constants for **2c** reaction with NAC at various pH

| pH | $k_2$ [$M^{-1}$ $s^{-1}$] |
|---|---|
| 7.0 | 9.9 ± 0.9 |
| 6.5 | 3.8 ± 0.7 |
| 6.0 | 2.0 ± 0.5 |

The reaction was followed in the solution of 50% DMSO and 100 mM Tris/HCl at 25 °C. The final concentration of **2c** and NAC was 20 μM and 1 mM, respectively.

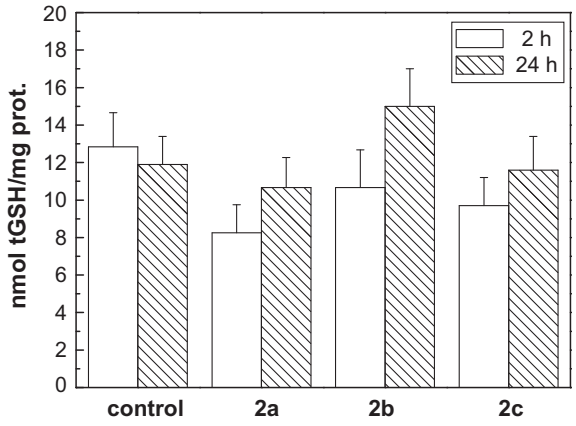


**Figure 7.** Glutathione in treated HL-60 cells. **2a** and **2b** (2 μM) and **2c** (1 μM) derivatives were incubated with cells for 2 h and for 24 h.

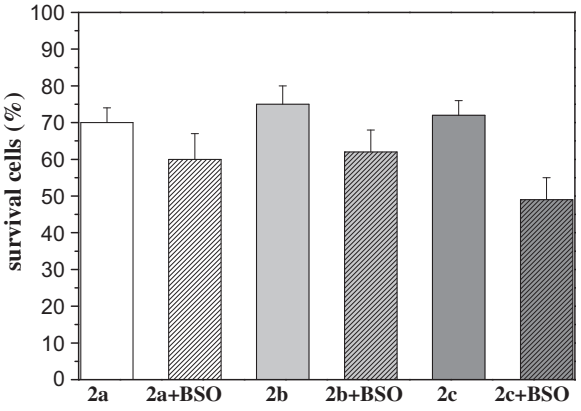


**Figure 8.** Cytotoxicity of **2a**–**2c** in BSO pretreated HL-60 cells. Cells were pretreated with BSO (10 μM) for 6 h and than incubated with **2a** (1.5 μM), **2b** (3.0 μM), and **2c** (1.0 μM), respectively, for 48 h. The number of viable cells was determined by trypan blue staining assay and the results are expressed as the percentage of all cells.

To determine the role of glutathione in cytotoxicity of **2a**–**2c**, HL-60 cells were pretreated with L-buthionine–sulfoximine (BSO). BSO application at concentration of 10 μM prior to **2a**–**2c** treatment induces a depletion of GSH by inhibition of γ-glutamylcysteine synthetase, a key enzyme active in glutathione biosynthesis. BSO itself exhibited no significant toxicity on HL-60 cells (data not shown). The results of trypan blue staining assay showed that BSO pre-treatment significantly augmented inhibition of the cell growth induced by three acridine–thiazolidinones (Fig. 8).

The depletion of intracellular glutathione can be associated with oxidative stress. Some acridine derivatives are able to induce oxidative stress. Blasiak et al.[5] found that free radicals may be involved in the formation of DNA lesions induced by amsacrine. We verified induction of oxidative stress in the presence of **2c.** Oxidative stress has been determined by DHE assay. The production of superoxide in **2c** (5 μM, 1 h) treated HL-60 cells has been confirmed (Fig. 9B), and when cells were pretreated with BSO (10 μM for 6 h), the generation of superoxide was enhanced in the presence of **2c** (Fig. 9C).

### 2.6. Arrest of cell cycle and cellular death

As interactions of compounds **2a**–**2c** with DNA and cellular thiols can induce a damage of cellular processes, an arrest of the cell cycle may be expected. We have really found that incubation of HL-60 cells with **2c** resulted in accumulation of cells in the $G_1$-phase of the cell cycle (Fig. 10), and the percentage of treated cells (1 μM **2c**, 48-h incubation) in the sub$G_0$ region (apoptotic cells) increased to 25%. The results show that low concentrations of **2c** can induce apoptosis (identified by a sub$G_0$ cell population).

To assess a type of cell death induced by higher concentration of **2a**–**c**, we analyzed their morphological changes after staining with propidium iodide (PI). Uptake of PI (red fluorescence) indicates a loss of membrane integrity, a characteristic hallmark of late apoptotic and necrotic cells. As seen in Figure 11, HL-60 cells treated with 5 μM **2a**–**2b** and 2.5 μM **2c** reduced their volume (cell shrinking) and were PI-positive after 24 h incubation.

Next studies (by dual FDA/PI fluorescent staining using FACS) showed that **2c** at concentration about 2 μM induced necrosis of cells (Fig. 12).

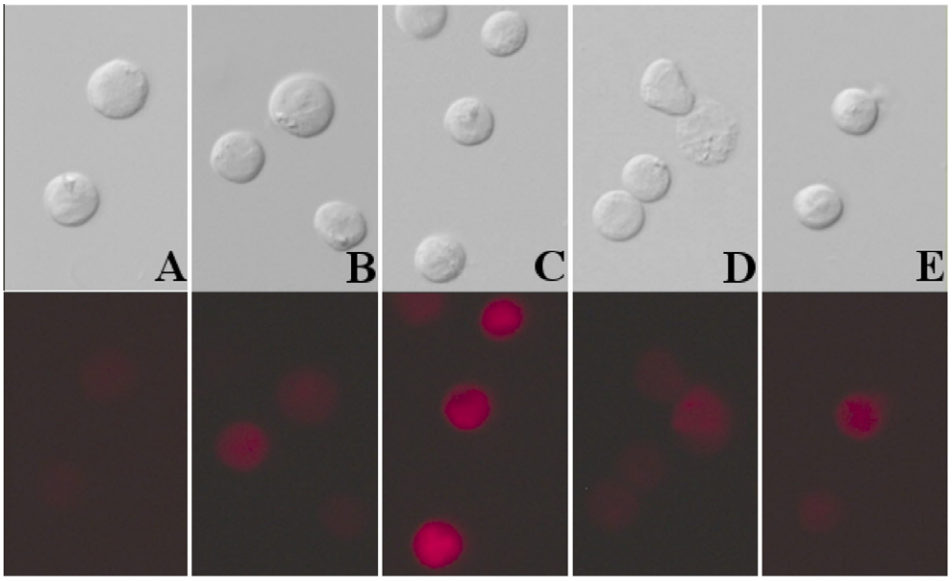


**Figure 9.** Oxidative stress induced by **2c** in human leukemia cells HL-60. Cells were incubated without **2c** (A, control), in the presence of 5 μM of **2c** for 1 h (B) or **2c** was added after pre-treatment with BSO (10 μM for 6 h, C). The positive control (D, menadione) and cells treated with BSO (E, 10 μM BSO for 6 h) are shown. Oxidative stress was assessed by the DHE assay, optical (upper) and fluorescence (lower) microphotographs, magnification 40 × 10.

| | $G_1$ [%] | $G_2$ [%] | S [%] | sub$G_0$ [%] |
|---|---|---|---|---|
| control | 48.14 | 12.90 | 38.96 | 1.93 |
| 0.5 μM **2c** | 51.04 | 10.56 | 38.4 | 21.70 |
| 1.0 μM **2c** | 82.93 | 5.08 | 11.99 | 25.85 |

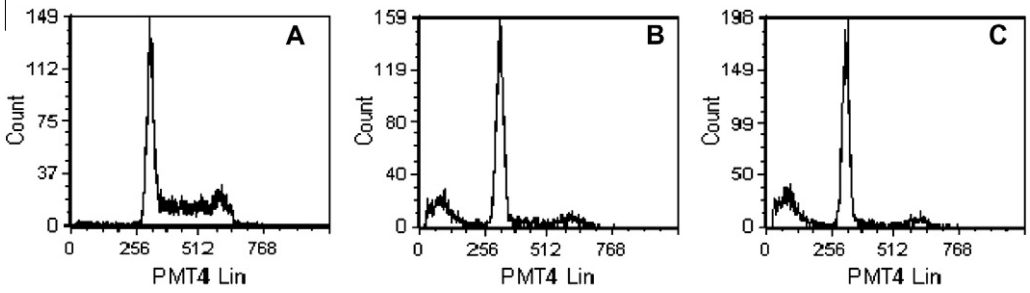


**Figure 10.** Analysis of cell cycle of HL-60 cells non-treated (A) and treated with **2c** (0.5 μM, B) and **2c** (1 μM, C) for 48 h. Analyses were performed with CANTO II as described in Section 4.3.

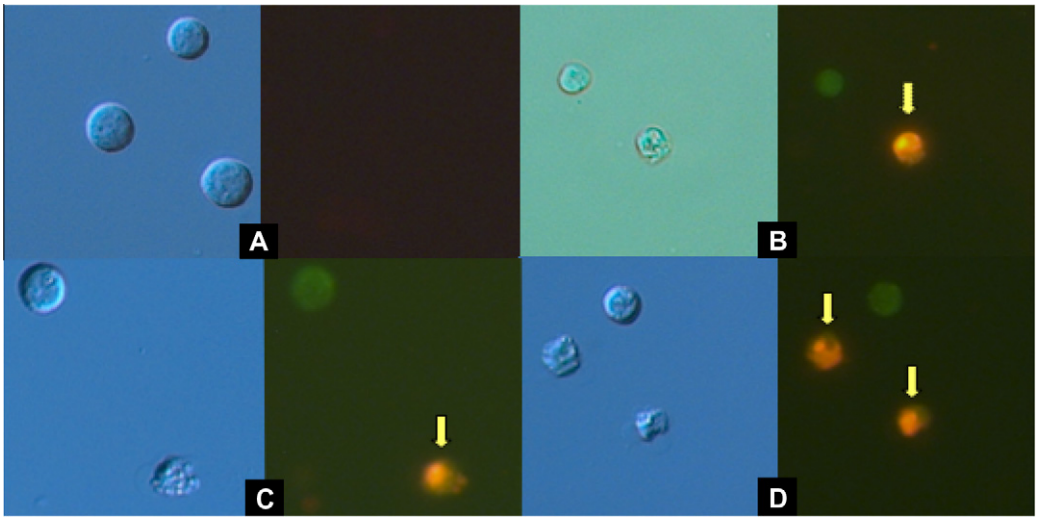


**Figure 11.** Microphotographs of HL-60 cells treated with 5 μM **2a** and **2b** (B, C) and 2.5 μM **2c** (D) for 24 h and non-treated cells (A). HL-60 cells were stained with PI (PI-positive marked with an arrow, magnification 40 × 10).

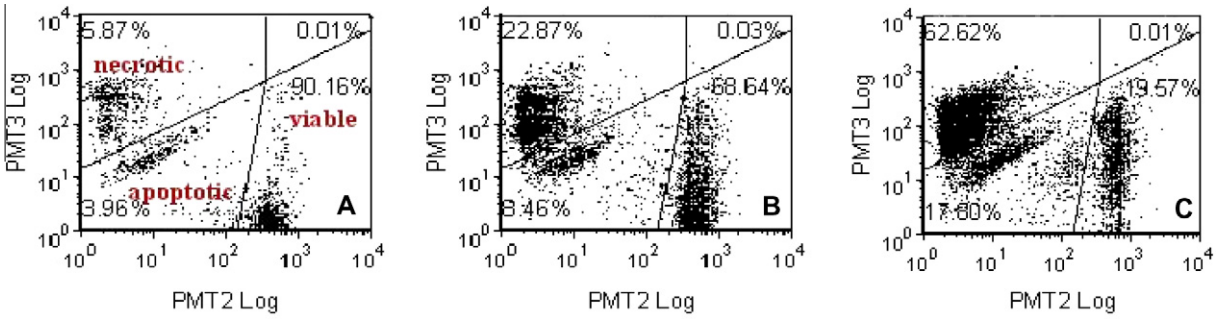


**Figure 12.** Analysis of cell death induced by 2 μM **2c** (B) and 4 μM **2c** (C) after 24 h incubation with HL-60 cells, nontreated cells (A). Cell death was detected by dual FDA/PI fluorescent staining using FACS.

## 3. Conclusion

New acridine–thiazolidinone derivatives **2a**–**2c** have shown the high affinity to calf thymus DNA with the binding constants *K* one order of magnitude greater than the *K* of daunomycin. All tested derivatives displayed a strong cytotoxic activity in vitro: they inhibited the growth of cancer cells and induced the cellular death at micromolar concentrations. The compounds also temporarily

changed the level of intracellular glutathione. The cytotoxicity of **2a**–**2c** seems to be associated with their DNA binding activity and the induction of oxidative stress. The new acridine–thiazolidinone substances may be inspiring for further development of DNA-targeted anticancer agents affecting also glutathione system of cells.

## 4. Experimental

### 4.1. Synthesis

NMR spectra were measured on a 400 MHz NMR spectrometer Varian Mercury Plus. IR spectra were obtained on a Specord IR 75 spectrophotometer and CHN analysis was carried out on a CHN analyzer Perkin–Elmer CHN 2400.

#### 4.1.1. Methyl 2-[2-(acridin-9-ylimino)-4-oxo-3-*sec*-butyl-1,3-thiazolan-5-yliden]acetate (2a)

Mp 175–177 °C, yield 57%. For $C_{23}H_{21}N_3O_3S$ (419.50) Calcd: 65.85% C, 5.05% H, 10.02% N. Found: 65.07% C, 4.90% H, 9.72% N; IR spectrum ($CHCl_3$): 1720 (ester C=O), 1693 (C=N), 1640 (amide C=O), 1613 (C=C). $^1$H NMR spectrum ($CDCl_3$, $\delta$): 1.15 (t, 3H, $^3J$ = 7.4 Hz, $CH_3$), 1.79 (d, 3H, $^3J$ = 6.9 Hz, $CH_3$), 2.25 (m, 2H, $CH_2$), 3.66 (s, 3H, $OCH_3$), 4.99 (sextet, 1H, $^3J$ = 6.9 Hz, CH), 6.90 (s, 1H, =CH), 7.47 (dd, 2H, $^3J$ = 8.6, 7.2 Hz, H-2′,7′), 7.78 (dd, 2H, $^3J$ = 8.4, 7.2 Hz, H-3′,6′), 7.80 (d, 2H, $^3J$ = 8.6 Hz, H-1′,8′), 8.23 (d, 2H, $^3J$ = 8.4 Hz, H-4′,5′).

#### 4.1.2. Methyl 2-[2-(acridin-9-ylimino)-4-oxo-3-*tert*-butyl-1,3-thiazolan-5-yliden]acetate (2b)

Mp 203–205 °C, yield 64%. For $C_{23}H_{21}N_3O_3S$ (419.50) Calcd: 65.85% C, 5.05% H, 10.02% N. Found: 65.62% C, 4.96% H, 9.95% N; IR spectrum ($CHCl_3$): 1726 (ester C=O), 1690 (C=N), 1640 (amide C=O), 1610 (C=C). $^1$H NMR spectrum ($CDCl_3$, $\delta$): 2.05 (s, 9H, $CH_3$), 3.64 (s, 3H, $OCH_3$), 6.82 (s, 1H, =CH), 7.49 (dd, 2H, $^3J$ = 8.6, 7.1 Hz, H-2′,7′), 7.79 (dd, 2H, $^3J$ = 8.8, 7.1 Hz, H-3′,6′), 7.83 (d, 2H, $^3J$ = 8.6 Hz, H-1′,8′), 8.27 (d, 2H, $^3J$ = 8.8 Hz, H-4′,5′).

#### 4.1.3. Methyl 2-[2-(acridin-9-ylimino)-3-(4-bromophenyl)-4-oxo-1,3-thiazolan-5-yliden]acetate (2c)

Mp 161–163 °C, yield 79%. For $C_{25}H_{16}BrN_3O_3S$ (518.40) Calcd: 57.92% C, 3.11% H, 8.11% N. Found: 57.49% C, 2.97% H, 7.95% N; IR spectrum ($CHCl_3$): 1726 (ester C=O), 1700 (C=N), 1643 (amide C=O), 1613 (C=C). $^1$H NMR spectrum ($CDCl_3$, $\delta$): 3.71 (s, 3H, $OCH_3$), 7.03 (s, 1H, =CH), 7.50 (ddd, 2H, $^3J$ = 8.4, 7.1 Hz, $^4J$ = 1.0 Hz, H-2′,7′), 7.55 (d, 2H, $^3J$ = 8.0 Hz, Ph), 7.78 (d, 2H, $^3J$ = 8.0 Hz, Ph), 7.79 (dd, 2H, $^3J$ = 8.2, 7.1 Hz, H-3′,6′), 7.88 (d, 2H, $^3J$ = 8.4 Hz, H-1′,8′), 8.26 (dd, 2H, $^3J$ = 8.2 Hz, $^4J$ = 1.0 Hz, H-4′,5′).

### 4.2. Materials

Propidium iodide (PI), Triton X-100, reduced form of glutathione (GSH), L-buthionine-sulfoximine (BSO), menadione, 3-(4,5-dimethylthiazol-2-yl)-2,5-diphenyltetrazolium bromide (MTT), Hoechst 33342, fluorescein diacetate (FDA), dihydroethidium (DHE), dimethyl sulfoxide (DMSO), DMEM and RPMI-1640 medium, trypsin, β-nicotinamide adenine dinucleotide 2′-phosphate reduced tetrasodium salt hydrate (NADPH), glutathione reductase from baker's yeast, plasmid pUC19 (2761 bp, *DH* 5α), cisplatin, agarose (type II No-A-6877), and calf thymus DNA were obtained from Sigma–Aldrich. EDTA and RNase A were purchased from Serva, 5,5-dithio-bis(2-nitrobenzoic acid) (DTNB) from Merck, *N*-acetyl-L-cysteine (NAC) and glutathione reductase from Calbiochem. Penicillin, streptomycin, and fetal bovine serum (FBS) were obtained from Grand Island Biological Co., USA, and all other chemicals from Lachema (Czech Republic).

### 4.3. Biological studies

#### 4.3.1. UV–vis absorption measurements

UV–vis spectra were measured on a Varian Cary 100 UV–vis spectrophotometer in 0.01 M Tris buffer (pH 7.4). A solution of the calf thymus DNA (ctDNA) in TE (Tris–EDTA) buffer was sonicated for 5 min and the DNA concentration was determined from its absorbance at 260 nm. The purity of DNA was determined by monitoring the value $A_{260}/A_{280}$. The concentration of DNA at 260 nm was expressed as base pairs ranged from 0 to 30 μM bp. The derivatives **2a**–**2c** were all dissolved in DMSO from which working solutions were prepared by dilution using 0.01 M Tris buffer to a final concentration 25 μM. All measurements were performed at 24 °C.

#### 4.3.2. Fluorescence measurements

Fluorescence was scanned on a Varian Cary Eclipse spectrofluorimeter with a 10 nm slit width for excitation and emission beams. Emission spectra were recorded in the region 410–470 nm using an excitation wavelength 384 nm. Fluorescence intensities are expressed in arbitrary units. Fluorescence titrations were conducted by adding increasing amounts of ctDNA directly into the cell containing the solution of compounds **2a**–**2c** ($c = 26.7 \times 10^{-6}$ M, 0.01 M Tris buffer, pH 7.4). The concentration range of DNA was 0−32 μM bp. All measurements were performed at 24 °C.

#### 4.3.3. $T_m$ measurements

Thermal denaturation studies were conducted using a Varian Cary Eclipse spectrophotometer equipped with a thermostatic cell holder. The temperature was controlled by a thermostatic bath (±0.1 °C). The absorbance at 260 nm was monitored for either ctDNA (10 μM) or a mixture of DNA with **2a**–**2c** (5 μM) in BPE buffer, pH 7.1 (6 mM $Na_2HPO_4$, 2 mM $NaH_2PO_4$, 1 mM EDTA), with a heating rate 1 °C/min. Melting temperatures were determined as a maximum of the first derivative plots of melting curves.

#### 4.3.4. Equilibrium binding titration

Binding affinities were calculated from absorbance spectra according to the method of McGhee and von Hippel using data points from the Scatchard plot. The binding data were fitted using GNU Octave 2.1.73 software.[29]

#### 4.3.5. Cell culture conditions

Human myeloid leukemia cell line HL-60, mouse leukemia cell line L1210, human ovarian carcinoma cell line A2780 were obtained from Dr. P. Ujhazy, Roswell Park Cancer Institute, Buffalo. The cell lines (HL-60, L1210 and A2780) were grown in RPMI 1640 medium supplemented with 10% FBS, penicillin (100 units/mL), and streptomycin (100 μg/mL). Medium for HL-60 and A2780 cell lines was supplemented also with 2 mM glutamine. The cells were maintained at 37 °C in a humidified 5% $CO_2$ atmosphere. NIH-3T3 mouse embryonic fibroblast cells were obtained from the American Type Culture Collection, Rockville, MD (USA). NIH-3T3 cells were routinely cultured in DMEM supplemented with 10% FBS, 2 mM L-glutamine, penicillin (100 μg/mL) and streptomycin (100 μg/ml) in 5% $CO_2$ at 37 °C.

**4.3.5.1. MTT-assay.** The viability of cells was determined in the presence of **2a**–**2c** (concentration in the range 0–30 μM) or absence of tested derivatives using a MTT microculture tetrazolium assay as described previously.[33]

**4.3.5.2. DCC.** The cell proliferation, growth curves, and cytotoxic potential of compounds were determined by a trypan blue dye exclusion test (DCC). For three-day experiments, cells were seeded ($1 \times 10^5$ cells/mL) in Petri dishes and tested substances (or 1% DMSO-control) were added after 24 h; then cell proliferation was checked after 24, 48, and 72 h. Growth curves were obtained and inhibitory concentrations, $IC_{50}$, were determined. All dye exclusion tests were made three times.

### 4.3.6. Fluorescence microscopy

HL-60 cells harvested in log phase were counted and seeded ($0.5 \times 10^6$/mL).

### 4.3.7. Intracellular accumulation of compounds

HL-60 cells were treated with **2a**–**2c**. After 4 or 24 h incubation at 37 °C in a humidified atmosphere of 5% $CO_2$ in air, the cells were washed in PBS and observed by an optical microscope and a fluorescence microscope (Axio Zeiss Imager A1, camera AxioCam Mrc). The cells without **2a**–**2c** (a control) were stained with 10 μM of Hoechst for 10 min than washed in PBS.

### 4.3.8. Analysis of necrosis

HL-60 cells were treated with **2a**–**2c** for 24 h. After incubation, the cells were washed with PBS, PI was added to a final concentration of 1 μg/mL, and cells were incubated for 10 min at room temperature. The samples were re-washed twice with PBS and observed by an optical microscope and a fluorescence microscope (Axio Zeiss Imager A1, camera AxioCam Mrc).

### 4.3.9. Flow cytometry—PI staining for cell cycle analysis

The control and drug-treated cells ($0.5 \times 10^6$/mL) with 0.5 and 1 μM **2c** for 48 h were harvested by centrifugation and permeabilized by detergent treatment (0.1% Triton X-100 in PBS) for 30 min. After incubation with RNAase (50 μg/mL) at 37 °C, DNA was stained with propidium iodide (50 μg/mL). Canto II flow cytometer (Becton-Dickinson Mountain View, CA, USA) was used for measurements according to the manufacturer instructions. Data were evaluated with FCS Express 4.0 (de Novo) software. Forward/side light scatter characteristics was used to exclude the cell debris from the analysis and lin/peak PMT4 for the discrimination of doublets.

### 4.3.10. Flow cytometry—FDA/PI staining for detection of apoptosis/necrosis

Apoptosis of HL-60 cell line treated with 2 and 4 μM **2c** for 24 h was detected with fluorescent staining using flow cytometry. From $2.5 \times 10^5$ to $5 \times 10^5$ cells of each sample were re-washed twice with PBS and the pellet was stained with fluorescein diacetate (200 μL of 10 nmol/L FDA, 30 min, 25 °C in the dark) and subsequently with 5 μL of 1 mg/mL PI. Forward and side scatter, red (PI) and green (FDA) fluorescence were measured by flow cytometry (Canto II, Becton-Dickinson) and analyzed by FCS Express 4.0 (de Novo) software.

### 4.3.11. Determination of cellular glutathione

Cellular glutathione was measured as described.[34] Briefly, $2 \times 10^6$ cells were incubated with different concentrations of **2a**–**2c** for the indicated time intervals, then harvested by centrifugation, and washed with PBS. The cell pellets were re-suspended in 450 μL of 1 mM EDTA and disrupted by freezing and thawing (two cycles), then 50 μL of 16% (w/v) sulfosalicilic acid was added. These suspensions were centrifuged, then the deproteinized supernatants were neutralized with $NaHCO_3$ and 150 mM sodium phosphate buffer (pH 7.6), and after centrifugation (5 min, 4 °C, 10,000×*g*), the supernatants (450 μL) were used for determination of total GSH (tGSH) by adding 20 μL of 5 mM NADPH, 20 μL of 10 mM DTNB, and 500 μL of 150 mM sodium phosphate buffer (pH 6.2). The assay was initiated by the addition of 10 μL of gluthatione reductase (470 U/mL). The rate of formation of 5-thio-2-nitrobenzoic acid was monitored spectrophotometrically at 412 nm (Specord 250, Analytic Jena). tGSH concentration values were calculated from a standard curve and expressed in nmol/mg prot. Protein concentrations were determined by a method of Lowry et al. using BSA as standard.[35]

### 4.3.12. Reactivity of 2c with NAC

Reactivity of **2c** with NAC was investigated in a system containing 100 mM Tris/HCl buffer (pH 6.0–7.0) containing 50% of DMSO at 25 °C. The kinetic measurements were performed under conditions for a pseudomonomolecular reaction and the reaction rates were measured spectrophotometrically on a Specord 250 (Analytic Jena). The rate constants ($k_2$ [$M^{-1}$ $s^{-1}$]) were calculated ($k' = k_2$[NAC], $k'$–pseudo-first-order rate constant) using the p$K_a$ values of *N*-acetyl-L-cysteine (p$K_a$ = 9.5).

### 4.3.13. RP-HPLC analysis of cellular uptake

ODS columns were used for HPLC analysis of acridine derivative.[36] The chromatographic separation of **2c** was achieved on a C18 column (Watrex, 250 × 4, Reprosil 100 C18 with 5 μm particle size) using degassed mobile phase—methanol and ammonium formate (MP: a mixture of methanol and 50 mM ammonium formate in the ratio of 80:20 (v/v), pH was adjusted to 4.5 with formic acid), the flow rate was 0.5 mL/min. The column temperature was maintained at 25 °C and the detection was carried out at 370 nm. The standard concentration was 1 nmol/20 μL (the injection volume was 20 μL). The amount of **2c** in the cells was quantified using methanol extraction and RP-HPLC analysis. The cell pellets were re-suspended in 100 μL of methanol and mixed for 10 min. The mixture was kept for 1 h at 4 °C. The tubes were then centrifuged at 6700×*g* for 15 min (4 °C) to pellet any solid material. The extract (20 μL) was injected into the HPLC system (LC–10AT pump, SPD–10Ai, UV–vis detector, Shimadzu, Japan).

### 4.3.14. Fluorescence detection of superoxide

Dihydroethidium (DHE) was used to estimate intracellular superoxide production in HL-60 cells.[38] Cells ($4 \times 10^5$) in medium were incubated for 24 h at 37 °C, then **2c** was applied without or in the presence of BSO (10 μM of BSO has been added 6 h before addition of **2c**). Influence of the compounds on the generation of free radicals was monitored after 1 h. DHE (20 μM) was added and incubated for 20 min at 37 °C. After incubation, the cells were washed in PBS and fluorescence was monitored with a fluorescent microscope (Axio Zeiss Imager A1, camera AxioCam Mrc).

## Acknowledgments

Financial support from the Slovak Grant Agency VEGA (Grants 1/0097/10, 2/0177/11 and 1/0672/11) and APVV-0282-10 are gratefully acknowledged.

## References and notes

1. Belmont, P.; Bosson, J.; Godet, T.; Tiano, M. *Anticancer Agents Med. Chem.* **2007**, *7*, 139.
2. Sebestik, J.; Hlavacek, J.; Stibor, I. *Curr. Protein Pept. Sci.* **2007**, *8*, 471.
3. Denny, W. A. *Curr. Med. Chem.* **2002**, *9*, 1655.
4. Ferguson, L. R.; Denny, W. A. *Mutat. Res.* **2007**, *623*, 14.
5. Blasiak, J.; Gloc, E.; Drzewoski, J.; Wozniak, K.; Zadrozny, M.; Skorski, T.; Pertynski, T. *Mutat. Res.* **2003**, *535*, 25.
6. Cholewinski, G.; Dzierzbicka, K.; Kolodziejczyk, A. M. *Pharmacol. Rep.* **2011**, *63*, 305.
7. Liu, Q.; Zhang, J.; Wang, M. Q.; Zhang, D. W.; Lu, Q. S.; Huang, Y.; Lin, H. H.; Yu, X. Q. *Eur. J. Med. Chem.* **2010**, *45*, 5302.
8. Chilin, A.; Marzaro, G.; Marzano, C.; Via, L. D.; Ferlin, M. G.; Pastorini, G.; Guiotto, A. *Bioorg. Med. Chem.* **2009**, *17*, 523.

9. Janovec, L.; Kožurková, M.; Sabolová, D.; Ungvarský, J.; Paulíková, H.; Plšíková, J.; Vantová, Z.; Imrich, J. *Bioorg. Med. Chem.* **2011**, *19*, 1790.
10. Vantová, Z.; Paulíková, H.; Sabolová, D.; Kožurková, M.; Sucháňová, M.; Janovec, L.; Kristian, P.; Imrich, J. *Int. J. Biol. Macromol.* **2009**, *45*, 174.
11. Bajdichová, M.; Paulíková, H.; Jakubíková, J.; Sabolová, D. *Neoplasma* **2007**, *54*, 463.
12. Janovec, L.; Sabolová, D.; Kožurková, M.; Paulíková, H.; Kristian, P.; Ungvarský, J.; Moravčíková, E.; Bajdichová, M.; Podhradský, D.; Imrich, J. *Bioconjugate Chem.* **2007**, *18*, 93.
13. Kožurková, M.; Sabolová, D.; Janovec, L.; Mikeš, J.; Kovaľ, J.; Ungvarský, J.; Štefanišinová, M.; Fedoročko, P.; Kristian, P.; Imrich, J. *Bioorg. Med. Chem.* **2008**, *16*, 3976.
14. Tomaščiková, J.; Imrich, J.; Danihel, I.; Böhm, S.; Kristian, P. *Collect. Czech. Chem. Commun.* **2007**, *72*, 347.
15. Tomaščiková, J.; Danihel, I.; Böhm, S.; Imrich, J.; Kristian, P.; Potočňák, I.; Čejka, J.; Klika, K. D. J. *Mol. Struct.* **2008**, *875*, 419.
16. Tomaščiková, J.; Imrich, J.; Danihel, I.; Böhm, S.; Kristian, P.; Pisarčíková, J.; Sabol, M.; Klika, K. D. *Molecules* **2008**, *13*, 501.
17. Imrich, J.; Tomaščiková, J.; Danihel, I.; Kristian, P.; Böhm, S.; Klika, K. D. *Heterocycles* **2010**, *80*, 489.
18. Schafer, F. Q.; Buettner, G. R. *Free Radic. Biol. Med.* **2001**, *30*, 1191.
19. Go, Y. M.; Jones, D. P. *Antioxid. Redox Signal.* **2010**, *13*, 489.
20. Pallardo, F. V.; Markovic, J.; Garcia, J. L.; Vina, J. *Mol. Aspects Med.* **2009**, *30*, 77.
21. Géci, I.; Valtamo, P.; Imrich, J.; Kivelä, H.; Kristian, P.; Pihlaja, K. *J. Heterocycl. Chem.* **2005**, *42*, 907.
22. Mazagová, D.; Kristian, P.; Suchár, G.; Imrich, J.; Antalík, M. *Collect. Czech. Chem. Commun.* **1994**, *59*, 2632.
23. Carlson, C. B.; Beal, P. A. *Bioorg. Med. Chem. Lett.* **2000**, *10*, 1979.
24. Delcros, J. G.; Tomasi, S.; Carrington, S.; Martin, B.; Renault, J.; Blagbrough, I. S.; Uriac, P. *J. Med. Chem.* **2002**, *45*, 5098.
25. Kumar, C. V.; Asuncion, E. H. *J. Am. Chem. Soc.* **1993**, *115*, 8547.
26. McGhee, J. D.; von Hippel, P. H. *J. Mol. Biol.* **1974**, *86*, 469.
27. Jenkins, T. C. In *Methods in Molecular Biology*; Fox, K. R., Ed.; Humana Press: Totowa, New Jersey, 1997; Vol. 90, p 195.
28. Perez-Flores, L.; Ruiz-Chica, A. J.; Delcros, J. G.; Sanchez-Jimenez, F. M.; Ramirez, F. J. *Spectrochim. Acta, Part A* **2008**, *69*, 1089.
29. Buša, J. In *Octave*; Technical University in Košice: Košice, 2006; Vol. 1,.
30. Cysyk, R. L.; Shoemaker, D.; Adamson, R. H. *Drug Metab. Dispos.* **1977**, *5*, 579.
31. Ketterer, B. *Mutat. Res.* **1988**, *202*, 343.
32. Kern, J. C.; Kehrer, J. P. *Front. Biosci.* **2005**, *10*, 1727.
33. Carmichael, J.; DeGraff, W. G.; Gazdar, A. F.; Minna, J. D.; Mitchell, J. B. *Cancer Res.* **1987**, *47*, 943.
34. Anderson, M. E. *Methods Enzymol.* **1985**, *113*, 548.
35. Lowry, O. H.; Rosebrough, N. J.; Farr, A. L.; Randall, R. J. *J. Biol. Chem.* **1951**, *193*, 265.
36. Lu, C.-S.; Mai, F.-D.; Wu, C.-W.; Wu, R.-J.; Chen, C.-C. *Dyes Pigm.* **2008**, *76*, 706.
37. Barros, F. W.; Silva, T. G.; da Rocha Pitta, M. G.; Bezerra, D. P.; Costa-Lotufo, L. V.; de Moraes, M. O.; Pessoa, C.; de Moura, M. A.; de Abreu, F. C.; de Lima Mdo, C.; Galdino, S. L.; Pitta Ida, R.; Goulart, M. O. *Bioorg. Med. Chem.* **2012**, *20*, 3533.
38. Zhao, H.; Joseph, J.; Fales, H. M.; Sokoloski, E. A.; Levine, R. L.; Vasquez-Vivar, J.; Kalyanaraman, B. *Proc. Natl. Acad. Sci. U.S.A.* **2005**, *102*, 5727.